Program Digest, 2019 IEEE International Ultrasonics Symposium (IUS)
Glasgow, Scotland, October 6-9, 2019

A Novel Two-Dimensional Displacement Estimation for Angled Shear Wave Elastography

Syed Ali Hasnain
Dept. of Electrical Engineering
Sukkur IBA University
Sukkur, Pakistan
alihasnain.mece17@iba-suk.edu.pk

Safeer Hyder
Dept. of Electrical Engineering
Sukkur IBA University
Sukkur, Pakistan
safeer.hyder@iba-suk.edu.pk

Luzhen Nie
School of Electronic and Electrical Engineering
Ultrasound Group, University of Leeds
Leeds, UK
elln@leeds.ac.uk

Asraf Mohamed Moubark
Center for Integrated Systems Engineering and Advanced Technologies
Uniersiti kebangsaan Malaysia
Bangi, Selangor, Malaysia
asraf@eng.ukm.my

Steven Freear
School of Electronic and Electrical Engineering
Ultrasound Group, University of Leeds
Leeds, UK
s.freear@leeds.ac.uk

***Abstract*—This study aimed to estimate angled tissue motion for shear wave compounding applications. Shear wave elastography produces the quantitative elasticity biomarker for assessing the health status of tissues. In sheer wave compounding, steered shear waves are generated with different angles, and individual angle elasticity maps are averaged to improve tissue stiffness reconstruction. When shear waves are steered and the tissue motion is generated in multiple directions, traditional one dimensional (1D) displacement estimation fails in capturing actual shear wave amplitude and direction. This study investigated the use of two dimensional (2D) kernel to track angular shear wave motion, which resulted in the underestimation of displacement values. Consequently, a new method named as 2D proposed (2D-P) was used to calculate both axial and lateral motion components separately using 1D axial and lateral kernels. Final results indicated that, the proposed scheme produced an average improvement of 2.01 μm and 4.4 μm compared with the 1D axial cross correlation and 2D cross correlation based methods, respectively.**

***Index Terms*—Shear Wave Elastography, shear Wave Compounding, 2D Speckle Tracking**

I. INTRODUCTION

Tissue stiffness has been practiced as a bio-marker for centuries by physicians because various diseases such as cancer, inflammation, and fibrosis, all contribute to altering elastic properties of tissues [1], [2]. Over the last decade, scientists have developed an imaging modality which creates images of spatial distribution of shear modulus by generating shear waves and measuring their propagation speed, named as shear wave elastography [3].

In B-mode imaging, spatial compounding techniques are widely used to improve B-mode image quality and speckle tracking [4]. In shear wave compounding, similar procedure was used by supersonic shear-wave imaging (SSI) and comb-push ultrasound shear wave elastography (CUSE), where shear wave fields were produced from multiple directions and individual elasticity maps were averaged to minimize random noise and to improve inclusion geometry reconstruction [5], [3]. In shear wave compounding, for zero angle push-beams, waves propagate laterally while corresponding motion vector is orthogonal to the propagation direction (axial direction), and eventually aligned with the imaging beam-axis. The challenge arises when steered shear waves are generated and it changes the direction of motion vector as well, creating both axial and lateral motion components [6], [3]. To estimate the angled motion vector, there are various methods proposed in the research for both blood-flow and few are proposed for elastography applications.

The strain elastography [7] also shares the similar challenge, and estimates displacement vectors using angular insonifications proposed by U. Techavipoo, *et al*. [8]. Another method proposed by the Tanter, *et al*. uses two differently angled insonifications from separate sub-apertures of the array, and estimates 2D tissue motion [9]. In blood flow estimation, the angle between the transmit beam and blood flow direction limits its velocity vector estimation accurately. Jensen *et al*. proposed the directional beamforming concept where transmit beams were aligned with the blood flow angle in the receiving mode by post-processing the RF data [10], [11]. Another solution proposed by S. Hyder *et al*. enable tracking beam angles aligned to the push-beam angles so that tracking beams were aligned with the tissue motion [12]. In this study, two different approaches for measuring both axial and lateral displacement components are investigated and results are produced using phantom based experimental study. In the first method, a 2D cross correlation-based scheme where 2D kernel is selected, while in the second method, the axial u_z and lateral u_y tissue motions are estimated using 1D kernels in axial and lateral dimensions and the final motion vector u is computed using Eq. 3. These two schemes are compared with the 1D axial estimation method. These techniques are presented graphically as shown in Fig. 1. For this paper, 2D-P terminology is used for the proposed method while 1D and 2D are used for conventional methods correlation-based.

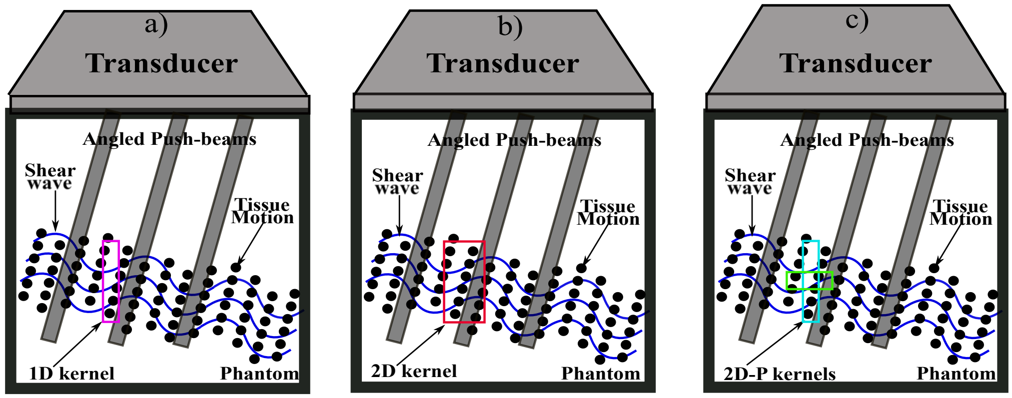

Fig. 1. The schematic diagram of displacement estimating scheme for angled shear wave with 1D axial kernel (1a), 2D kernel (1b), and 2D proposed kernels (1c). Gray bars indicate push-beam direction to generate angled shear waves, while shear waves direction is denoted by blue waves shown. In the 1D method, an axial kernel is selected, while 2D method use 2D data to produce both axial and lateral motion estimations. In the proposed 2D method, separately 1D axial and lateral tracking are used (1c) and both component values are used for calculating angled displacement vectors.

II. MATERIALS AND METHODS

A. Data Acquisition

Shear wave generation and tracking was achieved using a 128-element L3-8/40EP (Prosonic Co., Ltd, Korea) medical probe with a center frequency of 4.79 MHz. For data acquisition, the Ultrasound Research Array Platform II (UARP II) developed by the Ultrasound Group, University of Leeds was used [13], [14]. To create shear waves covering whole filed-of-view (FOV), three angled push-beams were used, where each was focused at 30-mm depth with sub-aperture of 16 elements and an inter-beam distance of 20 elements. Each push-beam was excited using a sinusoidal tone burst with a duration of 570 μs. Four different shear wave angles were investigated. A full 128-element plane aperture was used for receiving back-scattered RF data. A commercial multi-purpose, multi-tissue Zerdine gel-based ultrasound phantom (Model 040GSE, CIRS Inc., Norfolk, VA, USA) was used for all the experiments in this study. The acoustic speed of the phantom was 1540 m/s while ultrasound attenuation and density were 0.5 dB/cm/MHz and 1050 kg/m^3. For shear wave induced displacement tracking, coherent plane wave compounding was used to reduce random noise and improve B-mode imaging quality. Three different steering angles $(-2°, 0°, +2°)$ were used, therefore reducing frame-rate from 10 kHz to 3.33 KHz [4]. Beamforming of RF data was performed using the traditional delay-and-sum beamformer [15]. To increase the data sampling along the lateral dimension, RF data was beamformed with a lateral step size of 38.1 μm.

B. Displacement Motion Tracking Algorithm

The displacement estimation was performed after beamforming using three different techniques which included conventional 1D speckle tracking, conventional 2D speckle tracking, and proposed 2D displacement estimation. In the 1D method, an axial 1D kernel was selected from the B-mode frame, while the 2D based technique consisted of 2D kernels to estimate 2D motion vectors, respectively (see Fig. 1a and Fig. 1b). For the proposed technique, a separate 1D axial kernel and a 1D lateral kernel were used to estimate both axial and lateral components of the angled displacement vector (see Fig. 1c). For processing, the axial kernel was set to 2 mm while for the lateral dimension, a kernel size of 1.21 mm was selected, and for fair comparison, in all three techniques, similar size kernels were used, as applicable. Each kernel was shifted by 0.156 mm axially and 38.1 μm laterally, for successive estimations. To achieve sub-sample displacement estimation, both axial and lateral beamformed data was interpolated by 10 times using cubic interpolation. Before each correlation operation, data was smoothed using a hamming window. For both 1D and 2D displacement estimation, normalized cross correlation (NCC) was used as expressed using Eq. 1 and Eq. 2, respectively. In Eq. 1, f_r and f_s denote reference and shifted signals with M samples, while $\overline{f_r}$ and $\overline{f_s}$ indicate the mean of reference and shifted signals, respectively.

$$c(\tau_i) = \frac{\sum_{i=-M/2}^{M/2}[f_r(i) - \overline{f_r}][f_s(i+\tau_i) - \overline{f_s}(i)]}{\sqrt{\sum_{i=-M/2}^{M/2}[f_r(i) - \overline{f_r}]^2 \sum_{i=-M/2}^{M/2}[f_r(i+\tau_i) - \overline{f_s}(i)]^2}} \tag{1}$$

$$c(\tau_i, \tau_j) = \frac{\sum_{i=-M/2}^{M/2}\sum_{j=-N/2}^{N/2}[R][S]}{\sqrt{\sum_{i=-M/2}^{M/2}\sum_{j=-N/2}^{N/2}[R]^2 \sum_{i=-M/2}^{M/2}\sum_{j=-N/2}^{N/2}[S]^2}} \tag{2}$$

where $R = [f_r(i,j) - \overline{f_r}]$ and $S = [f_s(i+\tau_i, j+\tau_j) - \overline{f_s}(\tau_i, \tau_j)]$

$$u = \sqrt{(u_z)^2 + (u_x)^2} \tag{3}$$

where u is displacement vector, while u_z and u_x denote axial and lateral displacement components, respectively.

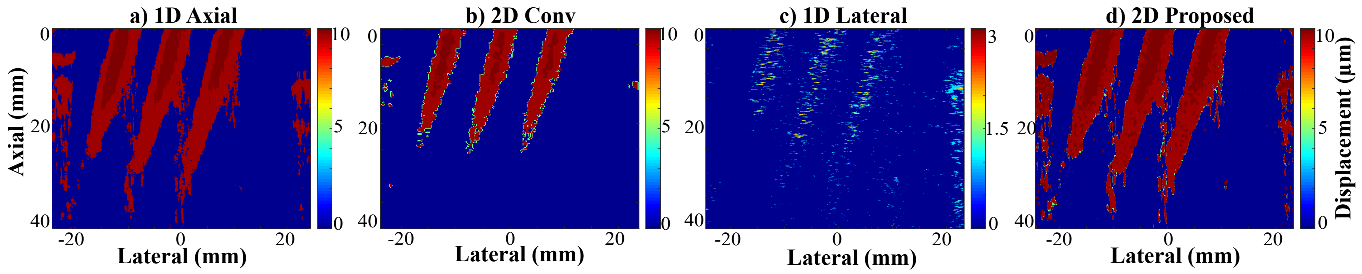

Fig. 2. The shear wave induced displacement maps are produced for -15° push-beam angle using displacement estimation methods as labeled on top of the each image. Displacement maps are processed using received RF data instantly after the push-beams are stopped and tracking beams are applied. It can be observed that, the 1D axial method produced images with noisy estimates between the push-beams, while the 2D conventional method removed the artifacts by averaging neighboring values due to a larger kernel size in the lateral direction. The Proposed scheme used axial and lateral displacement components separately, and calculated 2D displacement vector. The proposed technique is able to estimate the lateral displacement component which eventually improves displacement estimation.

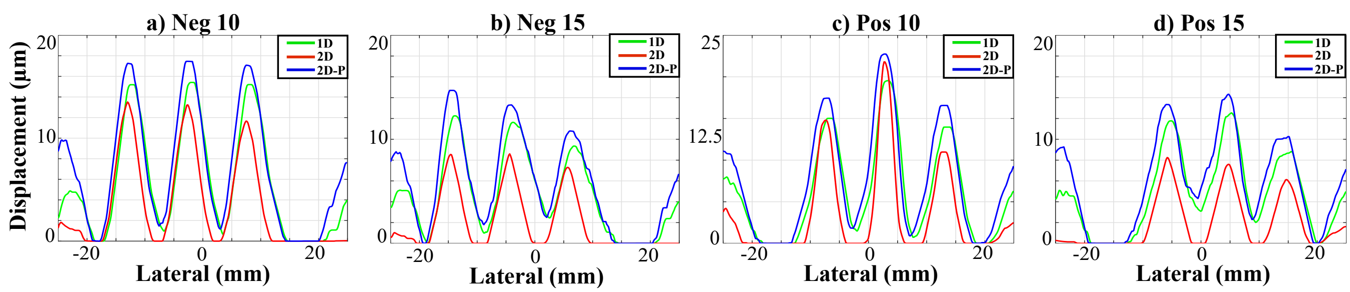

Fig. 3. Displacement amplitudes are plotted for 1D , 2D conventional and 2D proposed methods for each push beam $(-10^{\circ}, -15^{\circ}, +10^{\circ}, +15^{\circ})$ map in (a,b,c,d) plots, respectively. The displacement data is selected from a sub-frame with dimensions from 13 mm to 20 mm axially, all lateral points and then averaged along the axial direction. The proposed scheme produced an average improvement of 2.01 μm and 4.4 μm compared with the 1D axial cross-correlation and 2D cross-correction based methods, respectively.

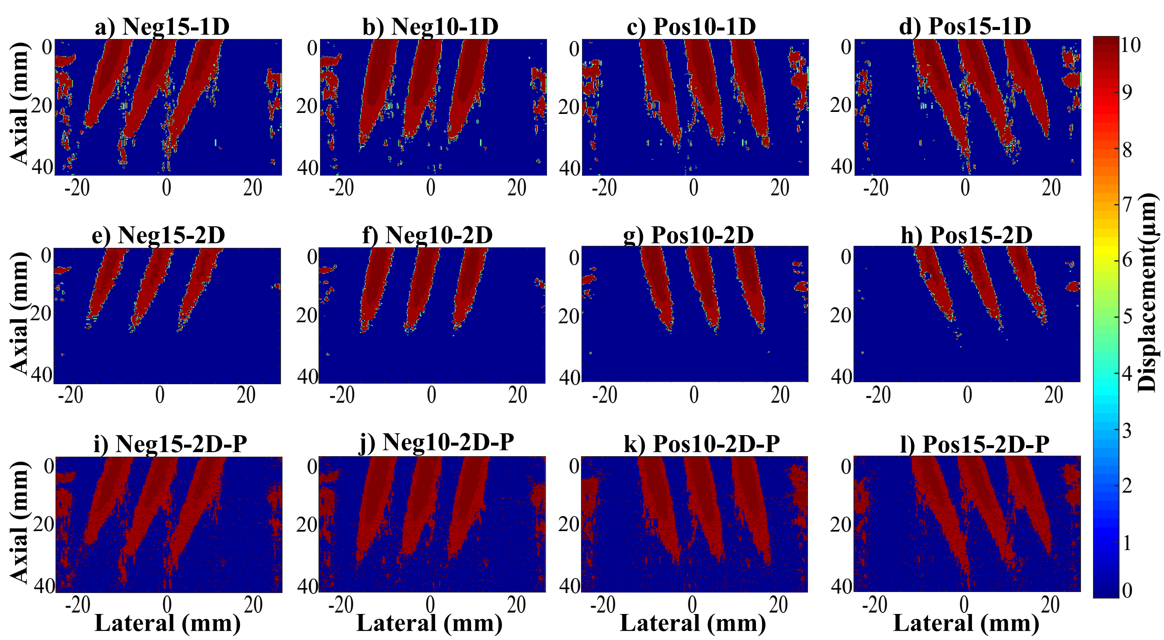

Fig. 4. Displacement maps for 1D, 2D full kernel and 2D proposed displacement estimation methods for push-beam angles as labeled on the images. The 1D axial method based images (a-d) produced inter-beam artifacts, simultaneously compromising on the lateral component of the displacement vector. Using the 2D kernel method (e-h), noise is fully suppressed at the push-beam contours but the displacement amplitude is reduced while the proposed 2D estimation method (i-l) is able to produce both axial and lateral components of displacements and improved the displacement vector amplitude effectively.

III. RESULTS AND DISCUSSION

This study aimed to calculate both axial and lateral components of the displacement vector for angled shear waves produced using angled push-beams. Two techniques were investigated in comparison with the existing 1D axial displacement scheme. The first technique used full 2D kernels for displacement estimation while in the second technique, a 1D axial and lateral kernel were used to separately calculate axial and transverse components. All these three techniques were explored for four different push-beams angles. According to the results, the 2D conventional scheme (see Fig. 2b) resulted in smaller displacement values compared with the 1D axial (see Fig. 2a) method, which was against the expectation. The reason of the reduction can be attributed to the lateral size of the kernel and the displacement profile (see Fig. 3) of the push-beam. As the shear wave generation beam contains the peak displacement at the center and attenuates as the measurement point travels away from the center laterally. This results in reduction of the peak displacement for 2D kernel-based scheme due to the averaging operation laterally. To reduce these effects, when using the proposed scheme, separate axial (see Fig. 2a) and lateral (see Fig. 2c) displacement components were estimated using 1D kernels and final motion vectors were calculated using Eq. 3 as shown in Fig. 2d. According to the results presented in Fig. 3, in terms of the amplitude of the displacement vector, the 2D proposed scheme performed better than both 1D axial and 2D conventional methods and results indicated performance consistency for all four push-beam angles. For four shear wave angles and three push-beams in each map, the peak displacement improvement values were averaged. The results indicated that the proposed scheme improved displacement upto 2.01 μm as compared to the 1D axial method and 4.4 μm as compared with the 2D conventional method. In terms of inter-beam artifacts, both 1D axial and 2D proposed performed equally while the conventional 2D scheme suppressed the artifacts completely and reconstructed the beam wavefront accurately. In this study, it was observed that, the 2D kernel-based cross-correlation does not accurately estimate the displacement amplitude due to the specific push-beam displacement profile while in strain elastography, motion is uniform within the 2D kernel dimensions. In future studies, the proposed scheme will be further optimized for the compound shear wave elastography application.

IV. CONCLUSION

In this experimental study, two different speckle tracking schemes were investigated for 2D tissue motion and the results were compared with the 1D-based schemes. The results concluded that, the conventional 2D schemes underestimated the motion values due to the Gaussian-curve like push beam displacement profile, while smoothing the inter-beam artifacts. Consequently upon the 2D conventional results, a new scheme was proposed, which calculated axial and lateral displacement components based on 1D cross-correlation and calculated final vector using both components. The proposed method estimated both axial and lateral motions and improved the final displacement amplitudes eventually. The results indicated that, the proposed scheme produced an improvement 2.01 μm and 4.4 μm compared with the 1D axial cross-correlation and 2D cross-correction based methods, respectively.

REFERENCES

[1] Ivan Z Nenadic, Matthew W Urban, James F Greenleaf, Jean-Luc Gennisson, Miguel Bernal, and Mickael Tanter. Ultrasound elastography for biomedical applications and medicine. 2019.

[2] Jeffrey Bamber, D Cosgrove, CF Dietrich, J Fromageau, J Bojunga, F Calliada, V Cantisani, J-M Correas, M Donofrio, EE Drakonaki, et al. Efsumb guidelines and recommendations on the clinical use of ultrasound elastography. part 1: Basic principles and technology. *Ultraschall in der Medizin-European Journal of Ultrasound*, 34(02):169–184, 2013.

[3] Jérémy Bercoff, Mickael Tanter, and Mathias Fink. Supersonic shear imaging: a new technique for soft tissue elasticity mapping. *IEEE Transactions on Ultrasonics, Ferroelectrics, and Frequency Control*, 51(4):396–409, 2004.

[4] Gabriel Montaldo, Mickaël Tanter, Jérémy Bercoff, Nicolas Benech, and Mathias Fink. Coherent plane-wave compounding for very high frame rate ultrasonography and transient elastography. *IEEE Transactions on Ultrasonics, Ferroelectrics, and Frequency Control*, 56(3):489–506, 2009.

[5] Pengfei Song, Armando Manduca, Heng Zhao, Matthew W Urban, James F Greenleaf, and Shigao Chen. Fast shear compounding using robust 2-d shear wave speed calculation and multi-directional filtering. *Ultrasound in medicine & biology*, 40(6):1343–1355, 2014.

[6] Pengfei Song, Heng Zhao, Armando Manduca, Matthew W Urban, James F Greenleaf, and Shigao Chen. Comb-push ultrasound shear elastography (cuse): a novel method for two-dimensional shear elasticity imaging of soft tissues. *IEEE Transactions on Medical Imaging*, 31(9):1821–1832, 2012.

[7] Safeer Hyder, Sevan Harput, Zainab Alomari, and Steven Freear. Two-way quality assessment approach for tumour detection using free-hand strain imaging. In *2014 IEEE International Ultrasonics Symposium*, pages 1853–1856. IEEE, 2014.

[8] Udomchai Techavipoo, Quan Chen, Tomy Varghese, and James A Zagzebski. Estimation of displacement vectors and strain tensors in elastography using angular insonifications. *IEEE Transactions on Medical Imaging*, 23(12):1479–1489, 2004.

[9] Mickaël Tanter, Jeremy Bercoff, Laurent Sandrin, and Mathias Fink. Ultrafast compound imaging for 2-d motion vector estimation: Application to transient elastography. *IEEE Transactions on Ultrasonics, Ferroelectrics, and Frequency Control*, 49(10):1363–1374, 2002.

[10] Jmrgcn A Jensen. Directional velocity estimation using focusing along the flow direction. i: Theory and simulation. *IEEE Transactions on Ultrasonics, Ferroelectrics, and Frequency Control*, 50(7):857–872, 2003.

[11] Jørgen Arendt Jensen and Rasmus Bjerngaard. Directional velocity estimation using focusing along the flow direction. ii: Experimental investigation. *IEEE Transactions on Ultrasonics, Ferroelectrics, and Frequency Control*, 50(7):873–880, 2003.

[12] Safeer Hyder, Sevan Harput, Zainab Alomari, David MJ Cowell, James McLaughlan, and Steven Freear. Improved shear wave-front reconstruction method by aligning imaging beam angles with shear-wave polarization: Applied for shear compounding application. In *2016 IEEE International Ultrasonics Symposium (IUS)*, pages 1–4. IEEE, 2016.

[13] Peter R Smith, David MJ Cowell, Benjamin Raiton, Chau Vo Ky, and Steven Freear. Ultrasound array transmitter architecture with high timing resolution using embedded phase-locked loops. *IEEE Transactions on Ultrasonics, Ferroelectrics, and Frequency Control*, 59(1):40–49, 2012.

[14] Peter R Smith, David MJ Cowell, and Steven Freear. Width-modulated square-wave pulses for ultrasound applications. *IEEE Transactions on Ultrasonics, Ferroelectrics, and Frequency Control*, 60(11):2244–2256, 2013.

[15] Zainab Alomari, Sevan Harput, Safeer Hyder, and Steven Freear. The effect of the transducer parameters on spatial resolution in plane-wave imaging. In *2015 IEEE International Ultrasonics Symposium (IUS)*, pages 1–4. IEEE, 2015.